Obesity causes Pgc-1α deficiency in the pancreas leading to marked Il-6 up-regulation via NF-κB in acute pancreatitis

Salvador Pérez[1]†, Sergio Rius-Pérez[1]†, Isabela Finamor[1], Pablo Martí-Andrés[1], Ignacio Prieto[2], Raquel García[2], María Monsalve[2], Juan Sastre[1*]

[1]Department of Physiology, Faculty of Pharmacy, University of Valencia,

Avda. Vicente Andrés Estellés s/n, 46100 Burjasot (Valencia), Spain

[2]Instituto de Investigaciones Biomédicas "Alberto Sols" (CSIC-UAM),

Arturo Duperier, 4, 28029-Madrid, Spain

† S. Pérez and S. Rius-Pérez are equal first authors

Correspondence to: Prof. Juan Sastre, Department of Physiology, School of Pharmacy, University of Valencia, Avda. Vicente Andres Estelles s/n, 46100 Burjasot (Valencia), Spain. Phone: 34-963543815. Fax: 34-96-3543395. E-mail: juan.sastre@uv.es

Conflicts of interest do not exist

Running title: PGC-1α deficiency up-regulates IL-6 via NF-κB in pancreatitis

ABSTRACT

Obesity is associated with local and systemic complications in acute pancreatitis. PPAR³ co-activator 1± (PGC-1±) is a transcriptional co-activator and master regulator of mitochondrial biogenesis that exhibits dysregulation in obese subjects. Our aims were 1) to study PGC-1α levels in pancreas from lean or obese rats and mice with acute pancreatitis; and 2) to determine the role of PGC-1α in the inflammatory response during acute pancreatitis elucidating the signaling pathways regulated by PGC-1α. Lean and obese Zucker rats and lean and obese C57BL6 mice were used first, and subsequently wild-type and PGC-1α knock-out (KO) mice with cerulein-induced pancreatitis were used to assess the inflammatory response and expression of target genes. *Ppargc1a* mRNA and protein levels were markedly down-regulated in pancreas of obese mice versus lean mice. PGC-1α protein levels increased in pancreas of lean mice with acute pancreatitis, but not in obese mice with pancreatitis. *Il6* mRNA levels were dramatically up-regulated in pancreas of PGC-1α KO mice after cerulein-induced pancreatitis in comparison with wild type mice with pancreatitis. Edema and the inflammatory infiltrate were more intense in pancreas from PGC-1α KO mice than in wild type mice. The lack of PGC-1α markedly enhanced nuclear translocation of phospho-p65 and recruitment of p65 to *Il6* promoter. PGC-1α bound phospho-p65 in pancreas during pancreatitis in wild type mice. Glutathione depletion in cerulein-induced pancreatitis was more severe in KO mice than in wild type mice. PGC-1α KO mice with pancreatitis, but not wild type mice, exhibited increased MPO activity in the lungs together with alveolar wall thickening and collapse, which were abrogated by blockade of

- -

the IL-6 receptor gp130 with LMT-28. In conclusion, obese rodents exhibit PGC-1α deficiency in the pancreas. PGC-1α acts as selective repressor of NF-κB towards IL-6 in pancreas. PGC-1α deficiency markedly enhanced NF-κB-mediated up-regulation of *Il6* in pancreas in pancreatitis, leading to severe inflammatory response.

INTRODUCTION

Obesity is a pro-inflammatory and epidemic condition associated with insulin resistance and metabolic syndrome [1,2]. In addition, obesity increases the risk of local and systemic complications and mortality in patients with acute pancreatitis [3–10], which has recently become the leading cause of hospitalization for gastrointestinal diseases [11]. Furthermore, necrotizing acute pancreatitis triggers higher expression of pro-inflammatory cytokines and mortality rate in obese rats than in controls [12,13]. Although some factors that contribute to the severe inflammatory response in obese patients or animals with pancreatitis have been unraveled, such as increased interleukin IL-18 levels [14], deficient adiponectin levels [15], and abundant pancreatitis-associated fat necrosis [16], the mechanisms behind this enhanced inflammation still remain to be completely elucidated. This prompted us to focus on PPAR³ co-activator 1± (PGC-1±), a master transcriptional regulator of mitochondrial biogenesis and oxidative metabolism, as it additionally exhibits anti-inflammatory properties and suffers dysregulation in obese animals and patients [2,17].

A relationship between PGC-1± and inflammation has been previously established in skeletal and smooth muscle as well as in endothelial cells [2]. Thus, higher levels of pro-

- -

inflammatory cytokines were found in muscle and blood from skeletal muscle–specific PGC-1± knockout mice [2,17]. In addition, the pro-inflammatory cytokine expression triggered by TNF-± was diminished by PGC-1± in C2C12 muscle cells [18]. PGC-1± also reduced VCAM-1 and MCP-1 expression triggered by TNF-± in human aortic smooth muscle and endothelial cells [19]. These anti-inflammatory effects of PGC-1± were ascribed to reduced nuclear factor-º B (NF-º B) activation through decreased phosphorylation of p65 and subsequently less transcriptional activity [2,18].

Taking into account the known impact of obesity on PGC-1± dysregulation that may affect the inflammatory cascade, our aims were 1) to study PGC-1± levels in pancreas from lean and obese mice with acute pancreatitis; and 2) to determine the role of PGC-1± in the inflammatory response during acute pancreatitis elucidating the signaling pathways regulated by PGC-1± that may affect the inflammatory response and tissue injury in this inflammatory disorder.

METHODS

Animals

Male lean Zucker (Lepr+/Lepr+) rats (318 ± 17 g; n=8) and obese Zucker (fa/fa) rats (418 ± 19 g; n=8) were purchased from Charles River (Barcelona, Spain). Lean Zucker rats are genetically identical to the obese Zucker rats used except for the leptin receptor mutation. They were fed a standard laboratory diet and tap water *ad libitum*.

C57BL/6J PGC-1α$^{-/-}$ mice were originally provided by Dr. Bruce Spiegelman (Dana-Farber Cancer Institute, Harvard Medical School, Boston, MA, USA) and following embryo transfer, a

- -

colony was established at the Institute of Biomedical Research "Alberto Sols" (Madrid, Spain) animal facility. Male C57BL/6J mice purchased from Jackson Laboratory (Bar Harbor, ME, USA) were used fed either standard chow (lean; 23,4 ± 1,0 g; n=10) or high fat diet with 60 % calories from fat (obese; 29.4 ± 1.2 g; n=10) for 12 weeks. Subsequently, male C57BL/6J PGC-1±$^{+/+}$ (23.1 ± 1.1 g; n=24) and C57BL/6J PGC-1±$^{-/-}$ (21.1 ± 1.7 g; n=24) mice as well as female C57BL/6J PGC-1±$^{+/+}$ (23.4 ± 1.7 g; n=9) and C57BL/6J PGC-1±$^{-/-}$ (20.8 ± 0.8 g; n=9) mice were used and fed standard diet. The generation and phenotype of PGC-1± knock-out (KO) mice were described previously [20].

All animals had tap water *ad libitum,* were housed at 20–22 °C and 50±10% humidity and were subjected to a 12 hour light-dark cycle. All animals received humane care according to the criteria outlined in the Guide for the Care and Use of Laboratory Animals (NIH publication 86-23 revised 1985). The study was approved by the Ethics Committee of Animal Experimentation and Welfare of the University of Valencia (Valencia, Spain).

Experimental model of acute pancreatitis

Taurocholate-induced acute pancreatitis was produced in Zucker rats. The biliopancreatic duct was cannulated through the duodenum and the hepatic duct was closed by a small bulldog clamp. Acute necrotizing pancreatitis was triggered by retrograde injection into the biliopancreatic duct of sodium taurocholate (3.5%) (Sigma-Aldrich, St. Louis, MO, USA) in a volume of 0.3 ml of 0.9% NaCl using an infusion pump (Harvard Apparatus, Holliston, MA, USA). Rats were sacrificed at 0 and 6 h after the infusion of taurocholate.

Cerulein-induced acute pancreatitis was performed in 12 week-old mice. Mice received seven intraperitoneal injections of cerulein (Sigma-Aldrich,) (50 µg/kg body weight) at 1 h intervals.

- -

Physiological saline was administered to the control group. For blockade of IL-6 receptors, the IL-6 antagonist LMT-28 (Sigma-Aldrich) (1 mg/kg, per oral) was administered 1 h before the first and fourth cerulein injections as described in [21]. LMT-28 targets the IL-6 Receptor ^{2} subunit, Glycoprotein 130 (gp130) [21]. LMT-28 was dissolved in 0.5% carboxymethyl cellulose (Sigma-Aldrich). Carboxymethyl cellulose (0.5%) was administered as vehicle. All animals were sacrificed 1 h after the last injection.

Animals were euthanized under anesthesia with Isothesia® (isoflurane) (Henry Schein Animal Health, Dublin, OH, USA) 3–5% and once they were unconscious they were exsanguinated and the pancreas and lungs immediately removed. Death was confirmed by cervical dislocation.

Determination of reduced glutathione (GSH) levels

Reduced glutathione (GSH) levels were determined in pancreas tissues spectrophotometrically at 340 nm using glutathione-S-transferase (Sigma-Aldrich) and 1-chloro-2,4-dinitrobenzene (Sigma-Aldrich) [22]. The homogenates were made in perchloric acid (Panreac, Barcelona, Spain) 6%, EDTA (Sigma-Aldrich) 1mM (100 mg tissue/ml).

Determination of malondialdehyde (MDA) levels

Lipid peroxidation was assessed by the measurement of MDA levels in pancreas tissue according to the HPLC method of Wong *et al* [23].

Myeloperoxidase (MPO)

MPO activity in lung was measured using tetramethylbenzidine (Sigma-Aldrich) as substrate in the presence of hydrogen peroxide [24].

- -

Antioxidant enzymes

To measure enzyme activities, pancreatic samples were homogenized in 50 mM potassium phosphate (pH 7.0), 1 mM EDTA (for catalase); in 20 mM HEPES (Sigma-Aldrich) (pH 7.2), 210 mM mannitol (Sigma-Aldrich), 70 mM sucrose (Sigma-Aldrich), 1 mM EGTA (Sigma-Aldrich) (for superoxide dismutase); in 50 mM Tris–HCl (pH 7.5), 1 mM DTT (Sigma-Aldrich), 5 mM EDTA (for glutathione peroxidase); and in 50 mM potassium phosphate (pH 7.4) (for glucose-6-phosphate dehydrogenase). Homogenates were centrifuged at 10,000 x *g* for 15 min, at 4 °C. Supernatants were used for enzyme activity determination. Catalase, superoxide dismutase, glutathione peroxidase and glucose 6-phosphate dehydrogenase activities were determined using the Catalase Assay Kit, Superoxide Dismutase Assay Kit, Glutathione Peroxidase Assay Kit, and Glucose-6-phosphate dehydrogenase Assay Kit (Cayman Chemical, Ann Arbor, MI, USA), respectively, following the manufacturer's protocols.

Plasma Il-6 levels

A mouse IL-6 Quantikine ELISA kit (M6000B, R&D systems, Minneapolis, MN, USA) was used to measure plasma IL-6 levels, following the indications of the kit. A monoclonal antibody specific for mouse IL-6 was pre-coated onto a microplate. The coefficient of variations (CVs) obtained for intra-assay precision were 3.5-6.7 %. The sensitivity was 1.6 pg/ml.

RT-qPCR

A small piece (approximately 30 mg) of pancreas was excised and immediately immersed in RNA-later solution (Thermo Fisher Scientific, Waltham, MA, USA) to stabilize the RNA. RT-qPCR was performed using an iQTM5 Multicolor Real-Time PCR Detection System

- -

(Biorad Laboratories, Hercules, CA, USA). PrimeScript RT Reagent Kit (Perfect Real Time) (Takara, Kusatsu, Japan) was used for cDNA generation following kit indications. 500 ng of RNA was used for reverse transcription using PrimeScript reserve transcriptase in 2 steps: 15 minutes at 37 ℃ and 5 s at 85 ℃. The specific primers used are shown in supplementary material, Table S1. The threshold cycle (CT) was determined and relative gene expression was expressed as follows: fold change= $2^{-”(”CT)}$, where ”CT = CT target – CT reference transcript, and ”(”CT) = ”CT treated - ”CT control. *TATA binding protein (Tbp)* was used as reference transcript.

Western blotting

Pancreatic tissues were frozen at -80° C until homogenization in extraction buffer (100 mg/ml) on ice. The extraction buffer contained 20 mM Tris-HCl (pH 7.5), 1 mM EDTA, 150 mM NaCl, 0.1% SDS, 1% Igepal® CA-630, 30 mM sodium pyrophosphate, 50 mM sodium fluoride, 50 µM sodium orthovanadate (all from Sigma-Aldrich), and a protease inhibitors cocktail (Sigma-Aldrich) at a concentration of 4 µl/ml.

The following antibodies were used: anti-PGC-1± (1/500) (2178, Cell Signaling Technology, Danvers, MA, USA), anti-GCLc (1/1000) (ab41463, Abcam, Cambridge, UK), anti-NF-ºB p65 (1/1000) (8242, Cell Signaling Technology), anti-phospho-NF-ºB p65 (Ser 536) (1/1000) (3039, Cell Signaling Technology), anti-histone 3 (1/1000) (ab5103, Abcam), anti-phospho-STAT3 (Tyr705) (1/1000) (9145, Cell Signaling Technology), anti-STAT3 (1/1000) (4904, Cell Signaling Technology) and anti-beta tubulin (1/1000) (ab7792, Abcam).

Chromatin immunoprecipitation (ChIP)

- -

EZ-Magna ChIP™ HiSens Chromatin Immunoprecipitation Kit (Millipore, Burlington, MA, USA) was used to immunoprecipitate DNA from frozen pancreatic tissues as described by the manufacturer. In brief, 37% formaldehyde was used to crosslink 100 mg of pancreas tissue for 10 minutes. Chromatin was isolated and sonicated for 35 min. Magnetic beads provided by the kit and antibodies against NF-ᵒB p65 subunit (Millipore) were used for immunoprecipitation. Immunoprecipitated DNA was analysed using qPCR. Primers were designed according to the consensus binding sequence for NF-ᵒB GGGACTTTCC [25] to assess the recruitment of p65 to the promoter region of *Il6*, *Tnf* and *Il1b* genes (supplementary material, Table S2). Immunoprecipitation without anti-NF-ᵒB p65 subunit antibody was performed as a negative control.

Co-immunoprecipitation

Protein-protein interactions were analyzed by co-immunoprecipitation experiments. Whole-cell extracts were prepared and subjected to immunoprecipitation with specific antibody against PGC-1± (sc-518025, Santa Cruz, Dallas, TX, USA) or a control normal mouse IgG as previously described [26]. The immunoprecipitates were assessed for presence of anti-phospho-NF-ᵒB p65 (Ser 536) (1/1000) (3039, Cell Signaling Technology), for levels of Lys acetylation (1/1000) (9441, Cell Signaling Technology) and for mouse Ig G (sc-2025, Santa Cruz) by western blotting with specific antibodies.

Histological analysis

- -

Pieces of pancreas and lung were rapidly removed, fixed in 4% paraformaldehyde (Sigma-Aldrich) for 24 h and embedded in paraffin (Sigma-Aldrich), sections were prepared at 4 µm using an automatic microtome, and then stained with hematoxylin (Sigma-Aldrich) and eosin (Sigma-Aldrich) for microscopic analysis. Pancreatic sections were assessed at 20x objective magnification over 10 separate fields for severity of pancreatitis by scoring for edema and inflammatory infiltrate according to the procedure of Van Laethem *et al.* [27].

Statistical Analysis

Results are expressed as mean ± standard deviation (SD). Statistical analysis was performed in two steps. One-way analysis of variance (ANOVA) was performed first. When the overall comparison of groups was significant, differences between individual groups were investigated by the Scheffé test. Statistical differences are indicated in Figure legends.

RESULTS

PGC-1± levels are markedly reduced in pancreas from obese rats and mice at basal conditions and in pancreatitis.

In order to assess whether PGC-1± plays a role in obesity and acute pancreatitis, our first approach was to measure its levels in pancreas from lean or obese rats and mice under basal conditions and in acute pancreatitis. *Ppargc1a* mRNA and PGC-1± protein levels were markedly down-regulated in pancreas of obese rats and mice under basal conditions in comparison with lean animals (Figure. 1A,B and densitometry in supplementary material,

- -

Figure S1A,B). Obese Zucker rats exhibited a marked reduction in PGC-1α levels at 6 h after taurocholate-induced pancreatitis when compared with lean Zucker rats (Figure 1A). We previously reported that obese rats with this model of taurocholate-induced pancreatitis exhibit more severe GSH depletion in pancreas as well as a dramatic increase in fat necrosis and enhanced myeloperoxidase activity in the lungs in comparison with lean rats [16,28]. PGC-1± protein levels increased in pancreas of lean mice with cerulein-induced pancreatitis when compared with sham mice, however PGC-1± levels did not increase in pancreas of obese mice with pancreatitis and they were even lower than those of obese sham mice (Figure 1B, and densitometry in supplementary material, Figure S1B). The histological analysis of the pancreas from obese mice with pancreatitis showed more injury than pancreas from control mice with pancreatitis (see supplementary material, Figure S1C). These results prompted us to assess the severity of acute pancreatitis in knock-out mice deficient in PGC-1±.

PGC-1± deficiency enhances pancreatic inflammation in acute pancreatitis

The intensity of pancreatic inflammation was assessed by histological analysis, which revealed that both edema and inflammatory infiltrate in pancreas were more intense in PGC-1± knock-out (KO) mice than in wild type mice (Figure 1C). Interestingly, even under basal conditions PGC-1± KO mice exhibited edema and inflammatory infiltrate in the pancreas, which were absent in wild type mice at basal conditions (Figure 1C). In addition, serum amylase and lipase activities were higher in PGC-1± KO mice than in wild type mice during acute pancreatitis (Figure 1D,E).

PGC-1± deficiency leads to NF-ºB activation, *Il6* up-regulation and recruitment of p65 to the *Il6* promoter in acute pancreatitis

- -

Il6 mRNA levels were dramatically increased (around 10-fold) in pancreas of PGC-1± KO male mice after cerulein-induced pancreatitis in comparison with wild type mice with pancreatitis (Fig 2A). In the case of female mice, the up-regulation of *Il6 mRNA* in pancreatitis was around 2-fold in PGC-1± KO mice versus wild type mice (supplementary material, Figure S2A). However, although *Tnf* and *Il1b* mRNAs were also up-regulated in pancreas upon induction of pancreatitis by cerulein, there were no significant differences between PGC-1± KO mice and wild type mice (Figure 2A and supplementary material, Figure S2A). In order to determine whether NF-ºB activation is involved in the induction of *Il6* upon PGC-1± deficiency, nuclear translocation of phospho-65 as well as its recruitment to the *Il6* promoter were studied in pancreas from PGC-1± KO mice and wild type mice in cerulein-induced pancreatitis. The lack of PGC-1± markedly enhanced nuclear translocation of phospho-p65 and also increased the recruitment of p65 to the *Il6* promoter, whereas its recruitment to the promoters of *Tnf* or *Il1b* were not significantly different between KO and wild-type mice (Figure 2B,C).

PGC-1± binds the phospho-p65 subunit of NF-ºB in the pancreas during pancreatitis

It was previously reported that the p65 subunit of NF-ºB constitutively binds PGC-1± in cardiac cells repressing PGC-1± activity towards its target genes [29]. Hence, we performed immunoprecipitation of PGC-1± to assess whether PGC-1± could form a complex with p65 and phospho-p65 in pancreas under basal conditions and in acute pancreatitis. According to our immunoprecipitation studies, PGC-1± was constitutively bound to p65 in pancreas under basal conditions and it is noteworthy that the levels of the complex formed by PGC-1± and phospho-p65 markedly increased during acute pancreatitis (Figure 2D, and controls for immunoprecipitation in supplementary material, Figure S3A).

- -

PGC-1± deficiency triggers down-regulation of antioxidant enzyme mRNAs in pancreas. Acute pancreatitis triggered PGC-1± acetylation and down-regulation of its target genes.

Taking into account the major role of PGC-1± in the regulation of antioxidant genes particularly in mitochondria, and the impact of reactive oxygen species (ROS) homeostasis on NF-ºB activity, the mRNA expression of mitochondrial superoxide dismutase (*Sod2*) and peroxiredoxin 3 (*Prdx3*) as well as catalase (*Cat*) were measured in pancreas of PGC-1± KO and wild type mice under basal conditions and during pancreatitis. As expected, the lack of PGC-1± triggered marked down-regulation of all *Sod2*, *Prdx3*, and *Cat* mRNAs under basal conditions (Figure 3A). Importantly, In cerulein-induced pancreatitis there was a remarkable decrease in the steady state levels of these three mRNAs only in wild type mice, but not in KO mice where mRNA levels were kept low upon pancreatitis similarly to basal conditions, suggesting that cerulein dependent downregulation of these genes may be associated with PGC-1α inactivation (Figure 3A). Furthermore, the activities of Mn^{2+}-dependent SOD2 and catalase were measured in the pancreas to assess the impact of their mRNA down-regulation, and the profile of these enzyme activities was similar to the mRNA expression. Indeed, SOD2 and catalase activities were much lower in pancreas of PGC-1± KO mice than in wild type mice, and these activities markedly decreased in pancreatitis only in wild type mice but not in KO mice (Figure 3B). These results therefore suggest that antioxidant defenses are reduced by cerulein, possibly through the inactivation of PGC-1α.

Taking into account that PGC-1α levels were induced by cerulein but its activity seemed to be reduced we decided to investigate the levels of PGC-1α acetylation. It has been previously described that in acute pancreatitis, inflammatory cues such as those triggered by cerulein can

- -

down-regulate sirtuins and their deacetylase activity [30], which potentially could lead to PGC-1± acetylation and inhibition [31], PGC-1± acetylation was assessed in pancreatitis. Figure 3C shows that the levels of PGC-1± acetylation increased in pancreatitis. The decrease in PGC-1± activity was confirmed by assessing the mRNA expression of cytochrome c, another target gene not related to antioxidant genes, which also markedly decrease in pancreatitis (supplementary material, Figure S3B). These results therefore support that PGC-1α inactivation by acetylation, drives the downregulation of antioxidant genes in response to cerulein-induced pancreatitis.

PGC-1± deficiency enhances glutathione depletion and lipid peroxidation in pancreas during pancreatitis

As the intensity of glutathione depletion in pancreas correlates with pancreatic damage in acute pancreatitis [22,32] and PGC-1± deficiency might have an impact on reduced glutathione (GSH) levels in pancreas, these levels were measured in PGC-1± KO and wild type mice. Under basal conditions there were no significant changes in pancreatic GSH levels upon PGC-1± deficiency, but glutathione depletion in cerulein-induced pancreatitis was much more intense in KO mice than in wild type mice (Figure 4A), supporting the relevance of PGC-1α antioxidant control.

To further elucidate the mechanism involved in glutathione depletion upon PGC-1± deficiency in pancreatitis, we also measured the activity of glucose 6-phosphate dehydrogenase (G6PDH), which provides the necessary NADPH reducing equivalents to maintain glutathione levels in the reduced form, as well as protein levels of the catalytic subunit of glutamate cysteine ligase, which catalyzes the rate limiting step in GSH synthesis. Similar to other antioxidants, G6PDH activity was markedly lower in pancreas of KO mice under basal conditions and also in

- -

pancreatitis when compared with wild type mice (Figure 4B). Furthermore, G6PDH activity decreased in pancreas from *wild type* mice upon pancreatitis when compared with basal conditions (Figure 4B). Importantly levels of the catalytic subunit of glutamate-cysteine ligase (GCLc) were up-regulated in pancreas of PGC-1± KO mice under basal conditions in comparison with wild type mice, consistent with an possibly elevated glutathione turn-over, and were dramatically diminished upon pancreatitis, particularly in PGC-1± KO mice, suggesting that PGC-1α plays also a role in keeping GCLc levels (Figure 4C).

The antioxidant defense related to GSH and NADPH was also assessed by measuring pancreatic glutathione peroxidase activity, which decreased not only upon PGC-1± deficiency but also upon pancreatitis in both groups (Figure 4D). The loss of glutathione peroxidase activity was dramatic in KO mice with pancreatitis (Figure 4D). The remarkable decreases in glutathione and glutathione related activities in pancreas of PGC-1± KO mice prompted us to assess their impact in lipid peroxidation. Consistently, malondialdehyde (MDA) levels as marker of lipid peroxidation were higher in pancreas of KO mice than in wild type mice during pancreatitis, with no significant changes in basal conditions (Figure 4E), a pattern similar to that observed for GSH level.

PGC-1± deficiency increases IL-6 plasma levels and pulmonary damage in pancreatitis

The systemic inflammatory response upon PGC-1± deficiency was evaluated by assessing plasma IL-6 levels as well as pulmonary inflammation and damage. Plasma IL-6 levels increased almost four-fold in PGC-1± KO mice with pancreatitis when compared with wild type mice with pancreatitis (Figure 5B). Accordingly, the STAT3 pathway, which is dependent on

- -

IL-6 levels, was also activated in pancreas PGC-1± KO mice with pancreatitis (supplementary material, Figure S4A).

MPO activity in lung tissue was measured as a marker of inflammatory infiltrate and it increased only in male or female PGC-1± KO mice with pancreatitis, but not in male or female wild type mice with pancreatitis (Fig. 5C and supplementary material, Figure S2D). Pulmonary damage was evaluated by histological analysis, which revealed generalized alveolar wall thickening and collapse in lungs from PGC-1± KO mice with pancreatitis, but rather low alveolar wall thickening and collapse in lungs from wild type mice with pancreatitis (Figure 5D). Moreover, blockade of the IL-6 receptor gp130 with LMT-28 abrogated the increase in pulmonary MPO in PGC-1α KO mice and ameliorated the pulmonary and pancreatic injury according to the histological analysis (Figures 5A,C,D). Furthermore, there was a correlation between plasma IL-6 levels and pulmonary MPO activity in wild type and PGC-1α knock out mice (supplementary material, Figure S4D).

It is noteworthy that plasma IL-6 levels and pancreatic *Il-6* mRNA levels were also elevated in obese mice, which exhibit PGC-1± deficiency in pancreas, in comparison with lean mice (supplementary material, Figure S4B).

- -

DISCUSSION

PGC-1± is a transcription co-activator that acts as master regulator of lipid and glucose oxidative metabolism, mitochondrial biogenesis, and detoxifying genes for ROS [2,29,33]. Thus, PGC-1± deficiency leads to a metabolic swift towards a more glycolytic metabolism, diminished expression of antioxidant enzymes, and enhanced ROS levels in different tissues [29,33]. PGC-1± is affected by inflammation because TNF-± decreased the expression of PGC-1± *in vitro* in cardiac AC16 cells and *in vivo* in the heart of mice overexpressing TNF-± [34,35], and also because lipopolysaccharide induced its rapid up-regulation but a long term down-regulation in different tissues such as heart, kidney, and liver [2,36]. Importantly, the repression of *Ppargc1a* gene expression under these conditions was rescued by NF-κB inhibition [34,37,38]. Furthermore, p65 constitutively binds to PGC-1± in human cardiac cells and mouse heart blocking its transcriptional activity and it is noteworthy that this binding was enhanced upon NF-κB activation induced by TNF-±. PGC-1± also modulates the expression of pro-inflammatory genes. Thus, PGC-1± markedly diminished the induction of TNF-±, IL-6 and macrophage inflammatory protein-1± triggered by TNF-± in the skeletal muscle cell line C2C12 [18]. PGC-1± repressed TNF-± expression induced by all different TLR agonists, whereas it only diminished the expression of IL-6 when stimulated with TLR1/2 or TLR4 agonists in skeletal muscle cells [18].

The present work highlights the key role of PGC-1± in the inflammatory response and tissue injury in acute pancreatitis, particularly in *Il6* up-regulation and in its severe form associated with obesity. Our results show that obesity in mice leads to marked PGC-1± down-regulation in pancreas. We may hypothesize that either hyper-methylation of the *Ppargc1a*

\- -

promoter [39] or down-regulation by increased fatty acid levels -particularly palmitate-, might be involved in the decrease in pancreatic PGC-1α levels in obese animals [40]. In severe taurocholate-induced pancreatitis in rats there was a decrease in PGC-1$\pm$ protein levels during pancreatitis even in lean rats, and in obese rats its levels were dramatically reduced, whereas in mice in cerulein-induced pancreatitis obesity abrogated the induction of PGC-1$\pm$. The lack of induction of PGC-1$\pm$ in taurocholate-induced pancreatitis might contribute to the enhanced severity of this experimental model. We previously reported that obese rats with this model of taurocholate-induced pancreatitis exhibit more severe GSH depletion in pancreas as well as enhanced myeloperoxidase activity in the lungs in comparison with lean rats [16,28]. Moreover, other authors previously reported an enhanced pulmonary inflammatory response in ob/ob mice with cerulein-induced pancreatitis in comparison with control mice [41].

The role of PGC-1$\pm$ deficiency in pancreatitis has been demonstrated here using PGC-1$\pm$ knock-out mice, which exhibit marked up-regulation of *Il6* in pancreas and an increase in circulating levels of Il-6 after induction of pancreatitis. NF-º B nuclear translocation and recruitment of p65 to the *Il6* promoter drives Il-6 up-regulation, which strikingly seems to be specific to this cytokine as no significant up-regulation was found for *Tnf* or *Il1b*. Thus, PGC-1$\pm$ selectively modulates NF-º B and seems to function as a specific NF-º B repressor towards Il-6 (see Figure 6). Furthermore, our results suggest that PGC-1$\pm$ binds p65 and phospho-p65 in the pancreas and the complex with the latter is much more abundant during pancreatitis, which restrains its transcriptional activity towards *Il6* (see Figure 6).

- -

The increase in circulating IL-6 levels would justify the systemic inflammatory response evidenced by pulmonary infiltrate and injury found in PGC-1± knock-out mice, in accordance with previous reports [42] and as explained below.

Importantly, the dramatic decrease in antioxidant defenses triggered by PGC-1α deficiency that results in overt oxidative stress in cerulein treated mice likely contributes to the inflammatory process, in particular to NF-$^{\circ}$B activation, and further promotes tissue damage.

Hence, the combined increase in IL-6 levels with pancreatic PGC-1± deficiency would explain the enhanced systemic inflammatory response and tissue injury in the disease when high serum IL-6 levels are found in patients and particularly in obese subjects.

Indeed, serum levels of IL-6 are considered a reliable marker for severity in acute pancreatitis [43,44] and so far IL-6 secretion during the early course of this disease has been considered controlled by NF-$^{\circ}$B mainly in recruited myeloid cells [45]. Accordingly, Il-6-knock-out mice exhibited reduced circulating levels of CXCL1, pulmonary inflammatory infiltrate, and acute lung injury during severe acute pancreatitis, whereas wild-type mice exhibited 40% mortality; and administration of recombinant IL-6 promoted acute lung injury and enhanced death rate [45].

L-6 belongs to the family of gp130 ligands and transmits its signals not only through binding to the ubiquitous gp130 receptor but also to its specific membrane-bound receptor IL-6R and to soluble IL-6R. Thus, IL-6 may activate STAT3 through two different mechanisms, either by binding to membrane receptors gp130 or IL-6R or by complexation with soluble IL-6R (sIL-6R), which is called IL-6 trans-signaling [45–47]. The IL-6/sIL-6R complexes require kinase Jak-2 to activate the transcription factor STAT3 through phosphorylation at Y705 [48,49] -as we

- -

report here- which contributes decisively to the systemic pro-inflammatory action of IL-6 through up-regulation of CXCL1. The systemic effects of secreted IL-6 in pancreatitis seem to be mediated by trans-signaling after complexation with soluble IL-6 receptor that triggered persistent and strong STAT3 phosphorylation in the pancreas and high circulating levels of neutrophil attractant CXCL1, which mediated leukocyte infiltrate into the lung and promoted acute lung injury [45]. Hence, the IL-6 trans-signaling/STAT3/CXCL1 pathway but not classical IL-6 signaling seems to mediate IL-6–dependent acute lung injury in acute pancreatitis [45]. Our findings assessing the blockade of the gp130 receptor confirm the fundamental role of Il-6 induction in the pulmonary inflammatory response in acute pancreatitis of PGC-1α deficient mice (see Figure 5). Moreover, upon PGC-1± deficiency IL-6 is associated with enhanced injury in the pancreas, likely due to the severe glutathione depletion together with the dramatic failure of G6PDH and the enzymatic antioxidant defenses.

Although it is well known that NF-ºB activation in pancreas is a major event during the early course of acute pancreatitis, its global impact is context-dependent as NF-ºB seems to be a double edge sword in this disease, depending on its basal activity, its short or long term transcriptional effects, the intensity of its activation, or the presence of specific co-activators or co-repressors, such as PGC-1± that selectively modulates its transcriptional activity towards Il-6. Although numerous studies during last decades highlight the key contribution of NF-ºB activation in pancreatic acinar cells to the local and systemic inflammatory response in acute pancreatitis including infection [50–57], more recent work has also shown a protective role of basal NF-ºB activity in pancreatic acinar cells [58,59]. Thus, selective deficiency of RelA in exocrine pancreas markedly aggravated acinar cell injury and death in acute pancreatitis also

- -

enhancing the systemic inflammatory response, particularly in the lung [58]. Moreover, constitutive and specific activation of NF-κB in exocrine pancreatic cells protects against acinar cell death and injury in acute pancreatitis by providing a preconditioning phenotype with up-regulation of protective PAP1 and Spi2a, the homologue of the human alpha1-antichymotrypsin [59]. In sum, our findings provide new insights into the regulation of NF-κB transcriptional activity by specific co-repressors, such as PGC-1α, and help to integrate and clarify the complex role of NF-κB within the context of the inflammatory process during acute pancreatitis, particularly in obesity.

In conclusion, the present work demonstrates the key role of PGC-1α in the inflammatory response in acute pancreatitis, particularly in its severe form associated with obesity. Obesity in mice leads to marked pancreatic PGC-1α down-regulation and abrogates the induction of PGC-1α during pancreatitis. Our results suggest that PGC-1α binds phospho-p65 acting as a selective repressor of NF-κB towards *Il6* in the pancreas. Thus, PGC-1α deficiency triggers NF-κB-mediated up-regulation of *Il6* in pancreas and an increase in Il-6 circulating levels during pancreatitis, leading to enhanced local and systemic inflammatory response. Hence, our results may unravel what's behind the elevated IL-6 levels as markers of severity in acute pancreatitis, and the combined increase in circulating IL-6 levels with pancreatic PGC-1α deficiency might explain the enhanced systemic inflammatory response and tissue injury in the disease when high serum IL-6 levels are found in patients, particularly in obese subjects.

Acknowledgments

- -

Author contributions statement

S.P, S.R.P and I.F. induced acute pancreatitis in mice. S.P, S.R.P., I.F. and P.M.A. performed most of the assays. S.P. performed the statistical analysis of the data. I.P. and R.G performed genotyping of the KO and wild type mice as well as histological analysis of pancreas and lung. S.R.P. prepared all figures of the manuscript. J.S. designed the study, supervised the experiments, and wrote the manuscript. M.M. provided the PGC-1± KO mice as well as important intellectual input and helped writing the manuscript.

References

1   Lumeng CN, Bodzin JL, Saltiel AR. Obesity induces a phenotypic switch in adipose tissue macrophage polarization. *J Clin Invest* 2007; **117:** 175–184

2   Eisele PS, Handschin C. Functional crosstalk of PGC-1 coactivators and inflammation in skeletal muscle pathophysiology. *Semin Immunopathol* 2014; **36:** 27–53

3   Wu BU, Banks PA. Clinical management of patients with acute pancreatitis. *Gastroenterology* 2013; **144:** 1272–1281

4   Martínez J, Johnson CD, Sánchez-Payá J, *et al.* Obesity is a definitive risk factor of severity and mortality in acute pancreatitis: an updated meta-analysis. *Pancreatology* 2006; **6:** 206–209

5   Porter KA, Banks PA. Obesity as a predictor of severity in acute pancreatitis. *Int J Pancreatol* 1991; **10:** 247–252

6   Martínez J, Sánchez-Payá J, Palazón JM, *et al.* Obesity: a prognostic factor of severity in acute pancreatitis. *Pancreas* 1999; **19:** 15–20

7   Papachristou GI, Papachristou DJ, Avula H, *et al.* Obesity increases the severity of acute pancreatitis: performance of APACHE-O score and correlation with the inflammatory response. *Pancreatology* 2006; **6:** 279–285

8   Sempere L, Martinez J, de Madaria E, *et al.* Obesity and fat distribution imply a greater systemic inflammatory response and a worse prognosis in acute pancreatitis. *Pancreatology* 2008; **8:** 257–264

9   Evans AC, Papachristou GI, Whitcomb DC. Obesity and the risk of severe acute pancreatitis. *Minerva Gastroenterol Dietol* 2010; **56:** 169–179

- -

10 O'Leary DP, O'Neill D, McLaughlin P, *et al.* Effects of abdominal fat distribution parameters on severity of acute pancreatitis. *World J Surg* 2012; **36:** 1679–1685

11 Peery AF, Crockett SD, Barritt AS, *et al.* Burden of gastrointestinal, liver, and pancreatic diseases in the United States. *Gastroenterology* 2015; **149:** 1731–1741.e3

12 Segersvärd R, Sylván M, Herrington M, *et al.* Obesity increases the severity of acute experimental pancreatitis in the rat. *Scand J Gastroenterol* 2001; **36:** 658–663

13 Segersvärd R, Tsai JA, Herrington MK, *et al.* Obesity alters cytokine gene expression and promotes liver injury in rats with acute pancreatitis. *Obes Silver Spring Md* 2008; **16:** 23–28

14 Sennello JA, Fayad R, Pini M, *et al.* Interleukin-18, together with interleukin-12, induces severe acute pancreatitis in obese but not in nonobese leptin-deficient mice. *Proc Natl Acad Sci U S A* 2008; **105:** 8085–8090

15 Araki H, Nishihara T, Matsuda M, *et al.* Adiponectin plays a protective role in caerulein-induced acute pancreatitis in mice fed a high-fat diet. *Gut* 2008; **57:** 1431–1440

16 Pereda J, Pérez S, Escobar J, *et al.* Obese rats exhibit high levels of fat necrosis and isoprostanes in taurocholate-induced acute pancreatitis. *PLoS One* 2012; **7:** e44383

17 Handschin C, Choi CS, Chin S, *et al.* Abnormal glucose homeostasis in skeletal muscle-specific PGC-1alpha knockout mice reveals skeletal muscle-pancreatic beta cell crosstalk. *J Clin Invest* 2007; **117:** 3463–3474

- -

18 Eisele PS, Salatino S, Sobek J, *et al.* The peroxisome proliferator-activated receptor ³ coactivator 1±/² (PGC-1) coactivators repress the transcriptional activity of NF-ºB in skeletal muscle cells. *J Biol Chem* 2013; **288:** 2246–2260

19 Kim H-J, Park K-G, Yoo E-K, *et al.* Effects of PGC-1alpha on TNF-alpha-induced MCP-1 and VCAM-1 expression and NF-kappaB activation in human aortic smooth muscle and endothelial cells. *Antioxid Redox Signal* 2007; **9:** 301–307

20 Lin J, Wu P-H, Tarr PT, *et al.* Defects in adaptive energy metabolism with CNS-linked hyperactivity in PGC-1alpha null mice. *Cell* 2004; **119:** 121–135

21 Hong S-S, Choi JH, Lee SY, *et al.* A novel small-molecule inhibitor targeting the IL-6 receptor ² subunit, Glycoprotein 130. *J Immunol* 2015; **195:** 237–245

22 Pereda J, Escobar J, Sandoval J, *et al.* Glutamate cysteine ligase up-regulation fails in necrotizing pancreatitis. *Free Radic Biol Med* 2008; **44:** 1599–1609

23 Wong SH, Knight JA, Hopfer SM, *et al.* Lipoperoxides in plasma as measured by liquid-chromatographic separation of malondialdehyde-thiobarbituric acid adduct. *Clin Chem* 1987; **33:** 214–220

24 Pérez S, Pereda J, Sabater L, *et al.* Pancreatic ascites hemoglobin contributes to the systemic response in acute pancreatitis. *Free Radic Biol Med* 2015; **81:** 145–155

25 Sen R, Baltimore D. Inducibility of kappa immunoglobulin enhancer-binding protein Nf-kappa B by a posttranslational mechanism. *Cell* 1986; **47:** 921–928

- -

26 Monsalve M, Wu Z, Adelmant G, *et al.* Direct coupling of transcription and mRNA processing through the thermogenic coactivator PGC-1. *Mol Cell* 2000; **6:** 307–316

27 Van Laethem JL, Eskinazi R, Louis H, *et al.* Multisystemic production of interleukin 10 limits the severity of acute pancreatitis in mice. *Gut* 1998; **43:** 408–413

28 Pérez S, Finamor I, Martí-Andrés P, *et al.* Role of obesity in the release of extracellular nucleosomes in acute pancreatitis: a clinical and experimental study. *Int J Obes (Lond)* 2018; doi: 10.1038/s41366-018-0073-6. [Epub ahead of print]

29 Alvarez-Guardia D, Palomer X, Coll T, *et al.* The p65 subunit of NF-kappaB binds to PGC-1alpha, linking inflammation and metabolic disturbances in cardiac cells. *Cardiovasc Res* 2010; **87:** 449–458

30 Shen A, Kim H-J, Oh G-S, *et al.* NAD+augmentation ameliorates acute pancreatitis through regulation of inflammasome signalling. *Sci Rep* 2017; **7:** 3006

31 Fernandez-Marcos PJ, Auwerx J. Regulation of PGC-1±, a nodal regulator of mitochondrial biogenesis. *Am J Clin Nutr* 2011; **93:** 884S–90

32 Neuschwander-Tetri BA, Ferrell LD, Sukhabote RJ, *et al.* Glutathione monoethyl ester ameliorates caerulein-induced pancreatitis in the mouse. *J Clin Invest* 1992; **89:** 109–116

33 St-Pierre J, Drori S, Uldry M, *et al.* Suppression of reactive oxygen species and neurodegeneration by the PGC-1 transcriptional coactivators. *Cell* 2006; **127:** 397–408

- -

34 Palomer X, Alvarez-Guardia D, Rodríguez-Calvo R, *et al.* TNF-alpha reduces PGC-1alpha expression through NF-kappaB and p38 MAPK leading to increased glucose oxidation in a human cardiac cell model. *Cardiovasc Res* 2009; **81:** 703–712

35 Adams RH, Porras A, Alonso G, *et al.* Essential role of p38alpha MAP kinase in placental but not embryonic cardiovascular development. *Mol Cell* 2000; **6:** 109–116

36 Yu XX, Barger JL, Boyer BB, *et al.* Impact of endotoxin on UCP homolog mRNA abundance, thermoregulation, and mitochondrial proton leak kinetics. *Am J Physiol Endocrinol Metab* 2000; **279:** E433–446

37 Feingold K, Kim MS, Shigenaga J, *et al.* Altered expression of nuclear hormone receptors and coactivators in mouse heart during the acute-phase response. *Am J Physiol Endocrinol Metab* 2004; **286:** E201–207

38 Planavila A, Sánchez RM, Merlos M, *et al.* Atorvastatin prevents peroxisome proliferator-activated receptor gamma coactivator-1 (PGC-1) downregulation in lipopolysaccharide-stimulated H9c2 cells. *Biochim Biophys Acta* 2005; **1736:** 120–127

39 Barrès R, Osler ME, Yan J, *et al.* Non-CpG methylation of the PGC-1alpha promoter through DNMT3B controls mitochondrial density. *Cell Metab* 2009; **10:** 189–198

40 Crunkhorn S, Dearie F, Mantzoros C, *et al.* Peroxisome proliferator activator receptor gamma coactivator-1 expression is reduced in obesity: potential pathogenic role of saturated fatty acids and p38 mitogen-activated protein kinase activation. *J Biol Chem* 2007; **282:** 15439–15450

41 Zyromski NJ, Mathur A, Pitt HA, *et al.* A murine model of obesity implicates the adipokine milieu in the pathogenesis of severe acute pancreatitis. *Am J Physiol Gastrointest Liver Physiol* 2008; **295:** G552–558

42 Kubota T, McTiernan CF, Frye CS, *et al.* Dilated cardiomyopathy in transgenic mice with cardiac-specific overexpression of tumor necrosis factor-alpha. *Circ Res* 1997; **81:** 627–635

43 Leser HG, Gross V, Scheibenbogen C, *et al.* Elevation of serum interleukin-6 concentration precedes acute-phase response and reflects severity in acute pancreatitis. *Gastroenterology* 1991; **101:** 782–785

44 Viedma JA, Pérez-Mateo M, Domínguez JE, *et al.* Role of interleukin-6 in acute pancreatitis. Comparison with C-reactive protein and phospholipase A. *Gut* 1992; **33:** 1264–1267

45 Zhang H, Neuhöfer P, Song L, *et al.* IL-6 trans-signaling promotes pancreatitis-associated lung injury and lethality. *J Clin Invest* 2013; **123:** 1019–1031

46 Jones SA, Richards PJ, Scheller J, *et al.* IL-6 transsignaling: the in vivo consequences. *J Interferon Cytokine Res* 2005; **25:** 241–253

47 Rabe B, Chalaris A, May U, *et al.* Transgenic blockade of interleukin 6 transsignaling abrogates inflammation. *Blood* 2008; **111:** 1021–1028

- -

48 Reipschläger S, Kubatzky K, Taromi S, *et al.* Toxin-induced RhoA activity mediates CCL1-triggered signal transducers and activators of transcription protein signaling. *J Biol Chem* 2012; **287:** 11183–11194

49 Birukova AA, Tian Y, Meliton A, *et al.* Stimulation of Rho signaling by pathologic mechanical stretch is a 'second hit' to Rho-independent lung injury induced by IL-6. *Am J Physiol Lung Cell Mol Physiol* 2012; **302:** L965–975

50 Gukovsky I, Gukovskaya AS, Blinman TA, *et al.* Early NF-kappaB activation is associated with hormone-induced pancreatitis. *Am J Physiol* 1998; **275:** G1402–1414

51 Steinle AU, Weidenbach H, Wagner M, *et al.* NF-kappaB/Rel activation in cerulein pancreatitis. *Gastroenterology* 1999; **116:** 420–430

52 Chen X, Ji B, Han B, *et al.* NF-kappaB activation in pancreas induces pancreatic and systemic inflammatory response. *Gastroenterology* 2002; **122:** 448–457

53 Aleksic T, Baumann B, Wagner M, *et al.* Cellular immune reaction in the pancreas is induced by constitutively active IkappaB kinase-2. *Gut* 2007; **56:** 227–236

54 Baumann B, Wagner M, Aleksic T, *et al.* Constitutive IKK2 activation in acinar cells is sufficient to induce pancreatitis in vivo. *J Clin Invest* 2007; **117:** 1502–1513

55 Hayashi T, Ishida Y, Kimura A, *et al.* IFN-gamma protects cerulein-induced acute pancreatitis by repressing NF-kappa B activation. *J Immunol* 2007; **178:** 7385–7394

- -

56 Rakonczay Z, Hegyi P, Takács T, *et al.* The role of NF-kappaB activation in the pathogenesis of acute pancreatitis. *Gut* 2008; **57:** 259–267

57 Sandoval J, Pereda J, Pérez S, *et al.* Epigenetic regulation of early- and late-response genes in acute pancreatitis. *J Immunol* 2016; **197:** 4137–4150

58 Algül H, Treiber M, Lesina M, *et al.* Pancreas-specific RelA/p65 truncation increases susceptibility of acini to inflammation-associated cell death following cerulein pancreatitis. *J Clin Invest* 2007; **117:** 1490–1501

59 Neuhöfer P, Liang S, Einwächter H, *et al.* Deletion of Iº B± activates RelA to reduce acute pancreatitis in mice through up-regulation of Spi2A. *Gastroenterology* 2013; **144:** 192–201

- -

FIGURE LEGENDS

Figure 1. Relative mRNA expression of *Ppargc1a* versus *Tbp* (*TATA binding protein*; housekeeping) in pancreas of male lean and obese Zucker rats; representative western blotting of PGC-1± in the pancreas of male lean and obese Zucker rats; and representative western blotting of PGC-1± in the pancreas of male lean and obese Zucker rats at 0h and 6 h after taurocholate-induced AP; ²-tubulin was used as loading control (A). mRNA relative expression of *Ppargc1a* versus *Tbp* in pancreas of male lean and obese mice; representative western blotting of PGC-1± in the pancreas of male lean and obese mice; and representative western blotting of PGC-1± in

- -

the pancreas of male sham lean and obese mice and at 1 h after cerulein-induced AP; β-tubulin was used as loading control (B). Representative histology and histological scores for edema and inflammatory infiltrate in pancreas of male sham C57BL/6J PGC-1$\pm^{+/+}$ (WT) and C57BL/6J PGC-1$\pm^{-/-}$ (KO) mice and at 1 h after cerulein-induced AP (C). Amylase (D) and pancreatic lipase (E) activities in plasma of male sham C57BL/6J PGC-1$\pm^{+/+}$ (WT) and C57BL/6J PGC-1$\pm^{-/-}$ (KO) mice and at 1 h after cerulein-induced AP. The number of rats per group was 4. The number of mice per group was 6. Results are expressed as mean ± SD. The statistical difference is indicated as follows: **P < 0.01.

- -

Figure 2. Relative expression of *Il6*, *Tnf* and *Il1b* versus *Tbp* (*TATA binding protein*) in pancreas of male sham C57BL/6J PGC-1±$^{+/+}$ (WT) and C57BL/6J PGC-1±$^{-/-}$ (KO) mice and at 1 h after cerulein-induced AP (A). Representative western blotting of nuclear levels of PGC-1±, phospho-p65 (Ser536) and p65 in pancreas of male C57BL/6J PGC-1±$^{+/+}$ (WT) and C57BL/6J

- -

PGC-1±$^{-/-}$ (KO) mice at 1 h after cerulein-induced AP; histone 3 (H3) was used as loading control (B). Histograms showing the recruitment of p65 in the promoter regions of *Il6*, *Tnf* and *Il1b* in pancreas of male C57BL/6J PGC-1±$^{+/+}$ (WT) and C57BL/6J PGC-1±$^{-/-}$ (KO) mice at 1 h after cerulein-induced AP mice measured by chromatin immunoprecipitation (ChIP) assay (C). Representative western blotting of phospho-p65 (Ser536) and p65 in PGC-1± immunoprecipitate of pancreas of male sham PGC1-±$^{+/+}$ (WT) mice and at 1 h after cerulein-induced AP mice; the immunoblot of IgG in PGC1-± immunoprecipitate was used as loading control (D). The number of mice per group was 6. The statistical difference is indicated as follows: *P < 0.05 and **P < 0.01.

- -

Figure 3. Relative mRNA expression of *Sod2*, *Cat* and *Prdx3* vs *Tbp* (*TATA binding protein*) in pancreas of male sham PGC1-±$^{+/+}$ (WT) and PGC1-±$^{-/-}$ (KO) mice and at 1 h after cerulein-induced AP (A). SOD2 and catalase activities in pancreas of male sham PGC1-±$^{+/+}$ (WT) and PGC1-±$^{-/-}$ (KO) mice and at 1 h after cerulein-induced AP mice (B). Representative western blotting of acetyl-lysine levels in PGC1-± immunoprecipitate of pancreas of male sham PGC1-±$^{+/+}$ (WT) mice and at 1 h after cerulein-induced AP mice. Immunoblot of IgG in PGC1-± immunoprecipitate was used as loading control (C). The number of mice per group was 6. The statistical difference is indicated as follows: *P < 0.05 and **P < 0.01.

- -

Figure 4. Levels of GSH in pancreas of male sham PGC1-$\pm^{+/+}$ (WT) and PGC1-$\pm^{-/-}$ (KO) mice and at 1 h after cerulein-induced AP (A). G6PDH activity in pancreas of male sham PGC1-$\pm^{+/+}$ (WT) and PGC1-$\pm^{-/-}$ (KO) mice and at 1 h after cerulein-induced AP (B). Representative western blotting of GCLc in pancreas of male sham PGC1-$\pm^{+/+}$ (WT) and PGC1-$\pm^{-/-}$ (KO) mice and at 1 h after cerulein-induced AP; ²-tubulin was used as loading control (C). Glutathione peroxidase (GPx) activity in pancreas of male sham PGC1-$\pm^{+/+}$ (WT) and PGC1-$\pm^{-/-}$ (KO) mice and at 1 h after cerulein-induced AP (D). Malondialdehyde (MDA) levels in pancreas of male sham PGC1-$\pm^{+/+}$ (WT) and PGC1-$\pm^{-/-}$ (KO) mice and at 1 h after cerulein-induced AP (E). The number of mice per group was 6. The statistical difference is indicated as follows: *P < 0.05 and **P < 0.01.

Figure 5. Representative histology and histological score for edema and inflammatory infiltrate in pancreas (A). Plasma IL-6 levels (B). Myeloperoxidase (MPO) activity in lung (C). Representative hematoxylin-eosin histological staining in lung (D) of male sham C57BL/6J PGC-1$\pm^{+/+}$ (WT) and C57BL/6J PGC-1$\pm^{-/-}$ (KO) mice, at 1 h after cerulein-induced AP, and at 1 h after AP with LMT-28 treatment. The number of mice per group was 5 to 6. The statistical difference is indicated as follows: *P < 0.05 and **P < 0.01.

Figure 6. PGC1$\pm$ acts as a selective repressor towards NF-κB-mediated expression of IL-6 in acute pancreatitis through binding phospho-p65 in a pancreatic acinar cell or infiltrating leukocyte.

- -

SUPPLEMENTARY MATERIAL ONLINE

Supplementary materials and methods YES

Supplementary figure legends YES

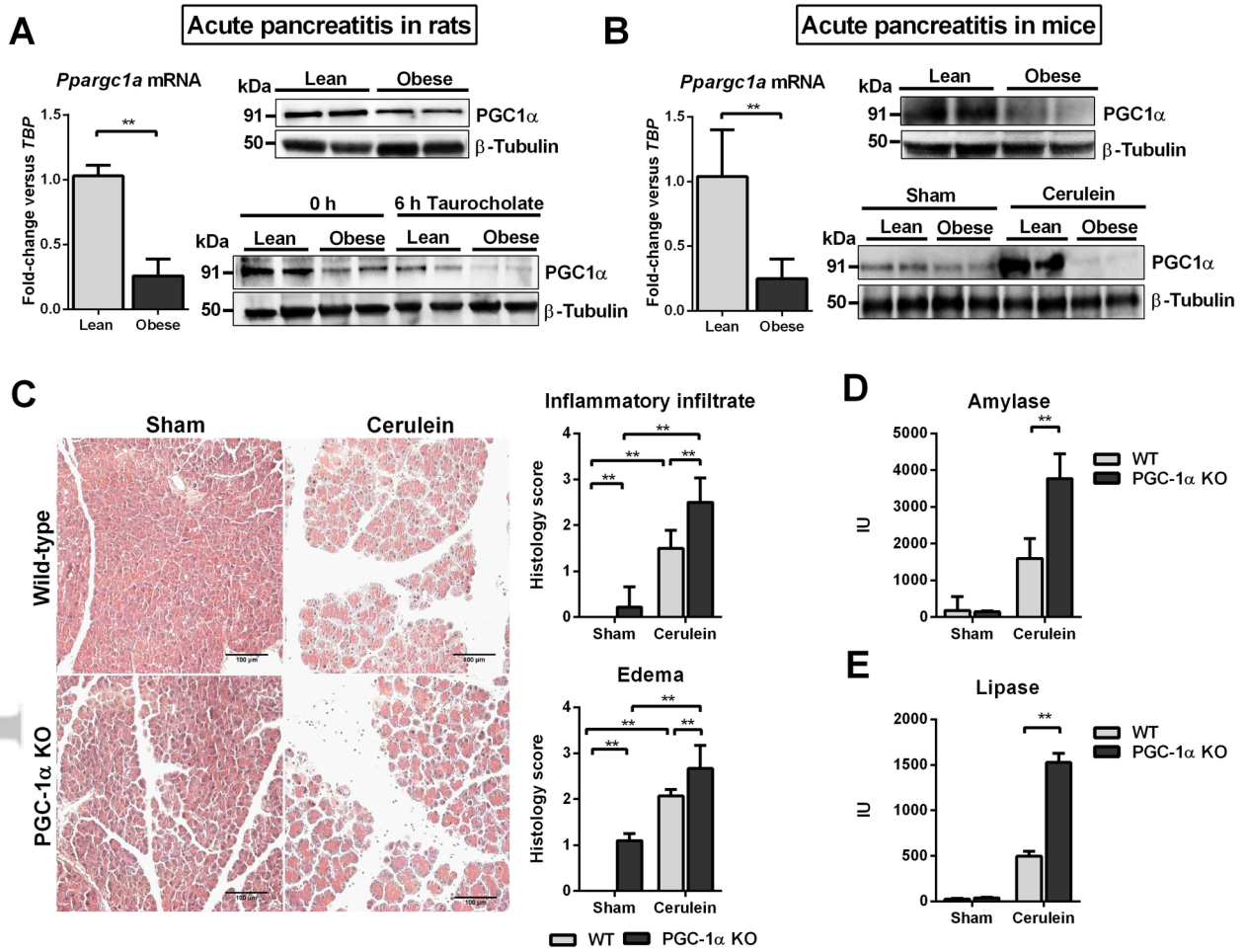**Figure S1.** Densitometric quantification of western blots

Figure S2. Relative expression of *Il6*, *Tnf* and *Il1b mRNAs* versus *Tbp* (TATA binding protein) mRNA in pancreas, western blotting of PGC-1± in pancreas and MPO activity in lung following treatment of WT and knockout mice.

Figure S3. Immunoblotting for PGC1-± in PGC1-± and non-specific IgG immunoprecipitation of pancreas and relative expression of *Cytc* versus *Tbp* mRNAs in the pancreas of male sham PGC1-±$^{+/+}$ wild type (WT) mice and WT mice at 1 h after cerulein-induced AP
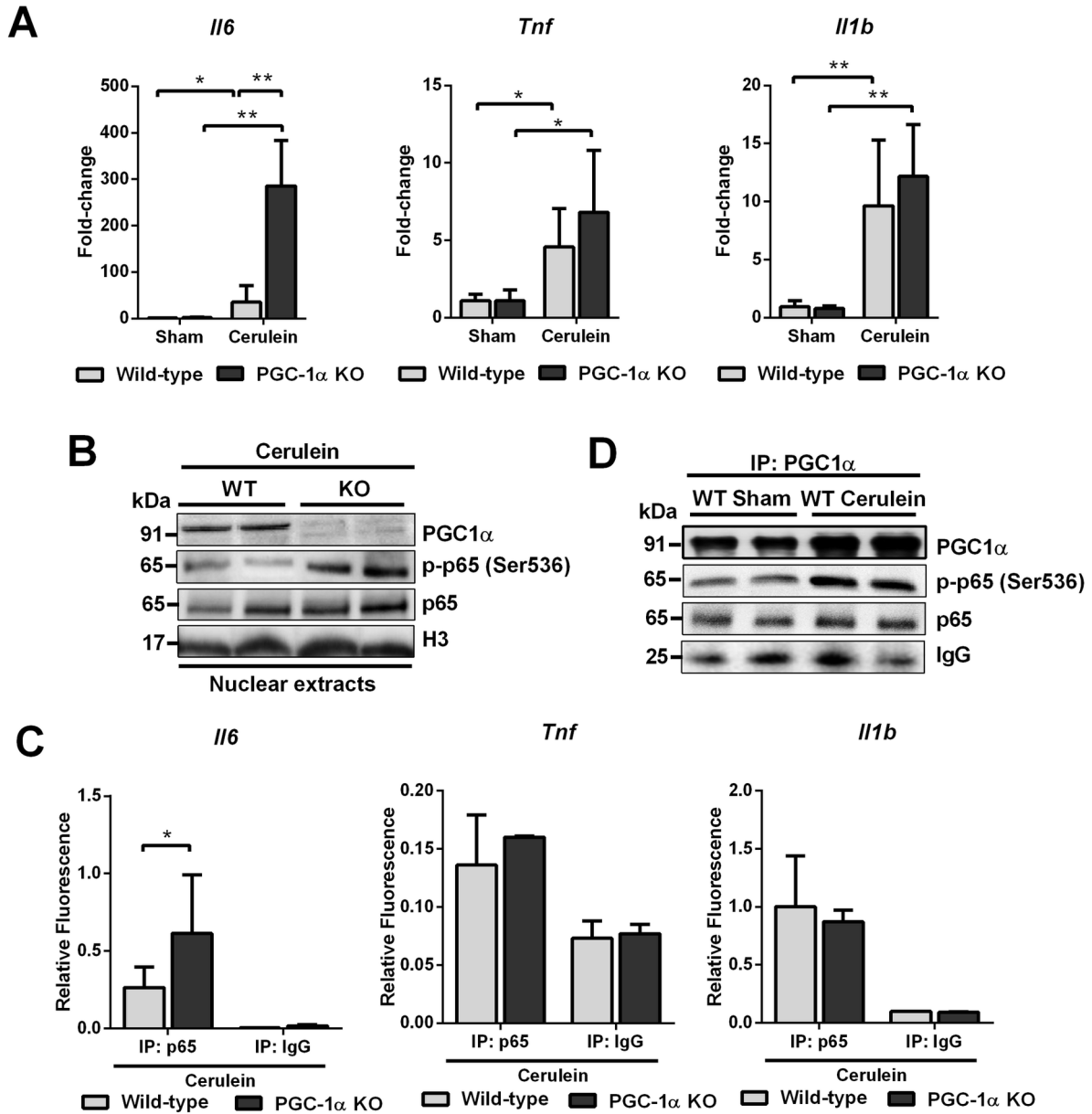
Figure S4. Representative western blotting of p-STAT3 (Y705) and STAT3, the relative expression of *Il6* mRNA, plasma Il-6 and the correlation between plasma Il-6 and pulmonary MPO levels

Table S1. Oligonucleotides used for RT-qPCR

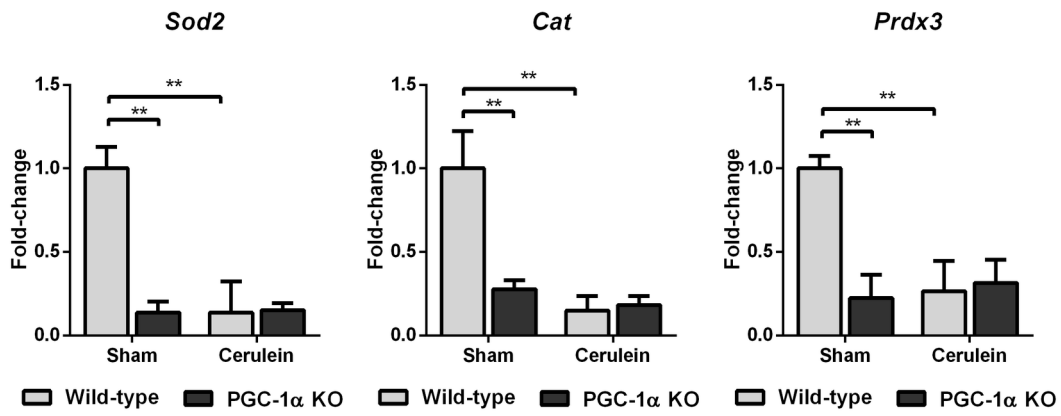**Table S2.** Oligonucleotides used for ChIP

- -

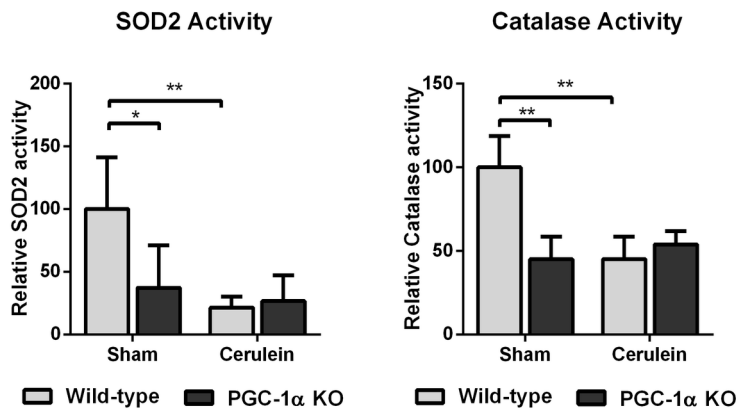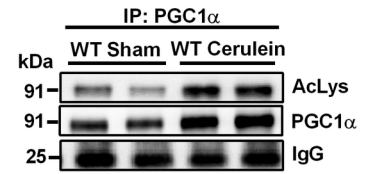**A** Acute pancreatitis in rats

Ppargc1a mRNA

B Acute pancreatitis in mice

Ppargc1a mRNA

C

Sham   Cerulein

Wild-type

PGC-1α KO

Inflammatory infiltrate

Edema

D Amylase

E Lipase

WT   PGC-1α KO
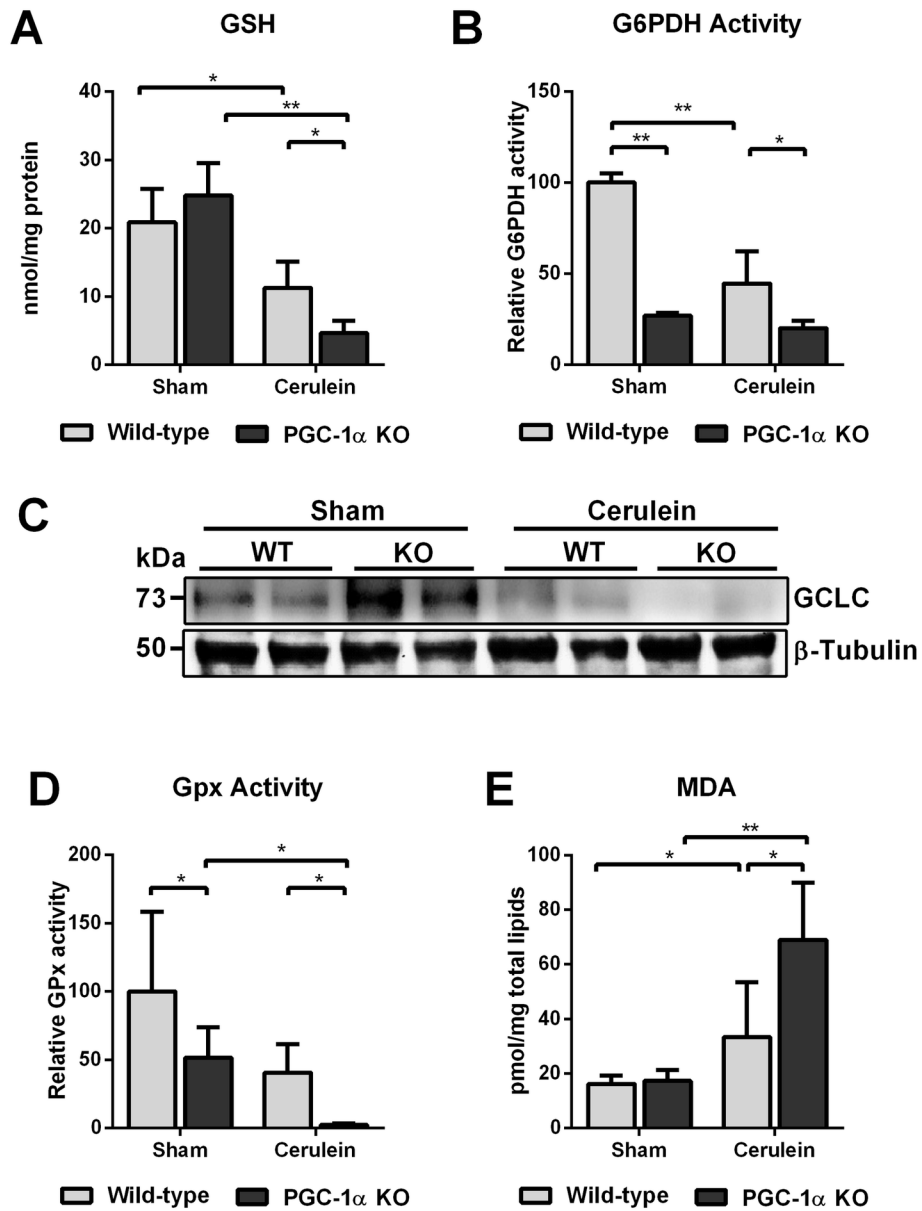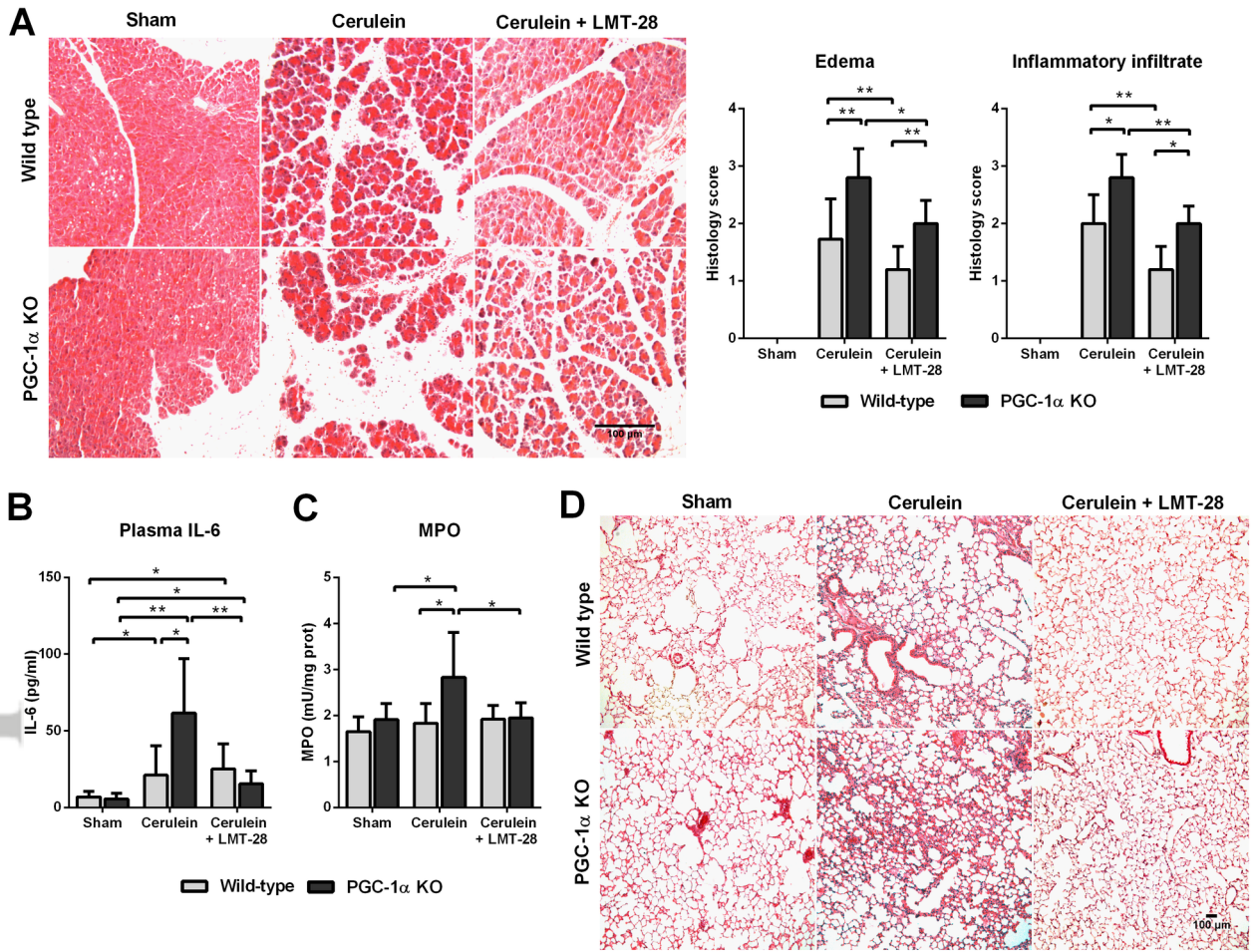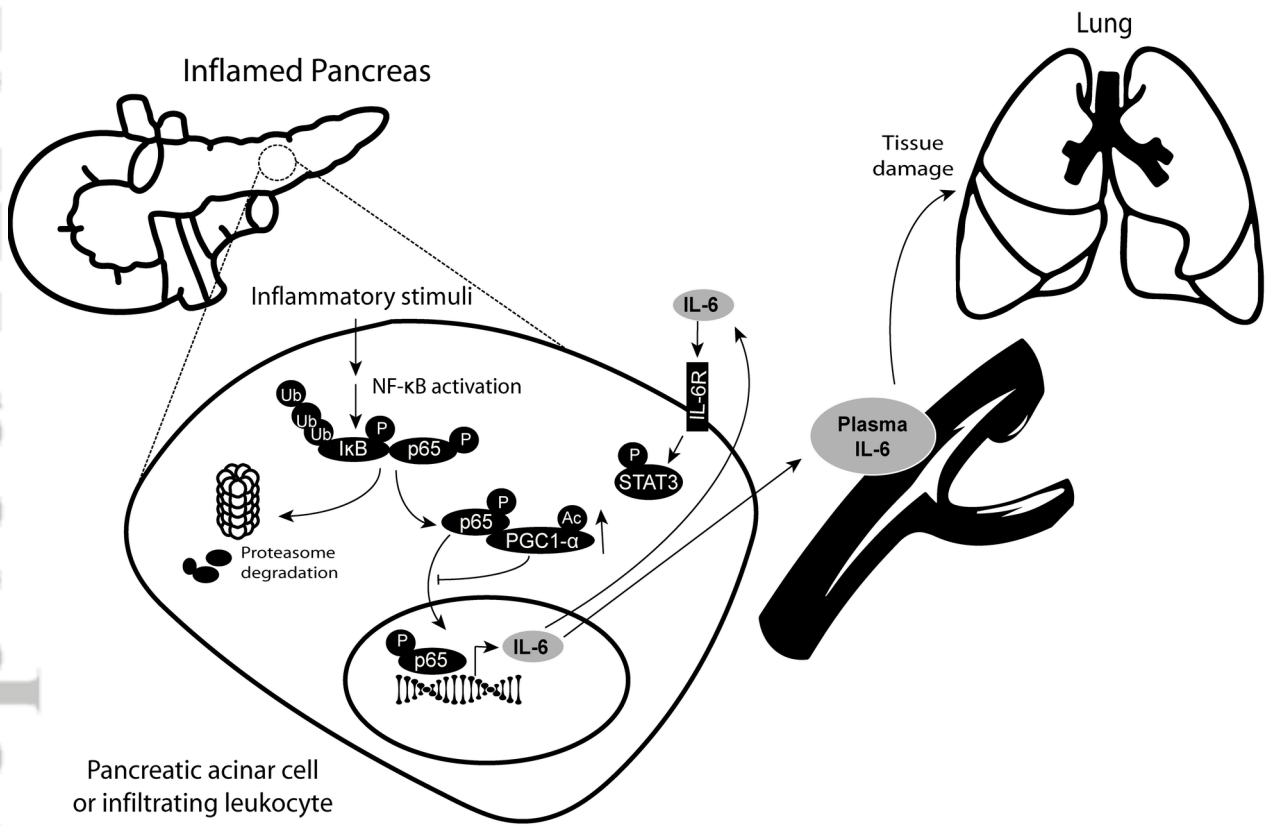
PATH_5166_F1.tif

PATH_5166_F2.tif

PATH_5166_F3.tif

PATH_5166_F4.tif

A

Sham Cerulein Cerulein + LMT-28

Wild type

PGC-1α KO

100 µm

Edema

Histology score

Inflammatory infiltrate

Histology score

Sham Cerulein Cerulein + LMT-28

☐ Wild-type ■ PGC-1α KO

B **Plasma IL-6**

IL-6 (pg/ml)

Sham Cerulein Cerulein + LMT-28

☐ Wild-type ■ PGC-1α KO

C **MPO**

MPO (mU/mg prot)

Sham Cerulein Cerulein + LMT-28

D

Sham Cerulein Cerulein + LMT-28

Wild type

PGC-1α KO

100 µm

PATH_5166_F5.tif

PATH_5166_F6.tif